Chemical control of convective instabilities

A. De Wit,

Nonlinear physical chemistry unit, Université Libre de Bruxelles, CP 231, 1050 Brussels, Belgium. Email: adewit@ulb.ac.be

Xxxx. Xxx. Xxx. Xxx. YYYY. AA:1–27

https://doi.org/10.1146/((please add article doi))

Keywords

reactive flows, viscous fingering, buoyancy-driven instabilities, Rayleigh-Taylor, double diffusion, chemical fronts

Abstract

By modifying a physical property of a solution like its density or viscosity, chemical reactions are able to influence and even trigger convective motions. These flows in turn affect the spatiotemporal distribution of the chemical species. A usually non trivial coupling between reactions and flows is then setting in. We present here simple model systems allowing to understand and analyze this chemo-hydrodynamic coupling. We illustrate in particular the possibility for chemical reactions to control or trigger viscous fingering, Rayleigh-Taylor, double diffusive, and convective dissolution instabilities. We discuss laboratory experiments performed to study these phenomena and compare the experimental results to theoretical predictions. We insist in each case on the specificities of the chemo-hydrodynamic patterns and instabilities with regard to those that develop in non reactive systems and unify the different dynamics in terms of the common features of the related spatial mobility profiles.

Contents

1. INTRODUCTION

Hydrodynamic instabilities of miscible interfaces are encountered in lots of applications where two fluids are put in contact. They typically develop when gradients of a physical property is present across the interface. As an example, a Rayleigh-Taylor instability can deform the miscible contact line into alternating rising and sinking fingers when a denser solution is put on top of a less dense one in the gravity field. Similarly, a viscous fingering instability can develop when a less viscous fluid displaces a more viscous one in a porous medium. Such instabilities have been much studied both experimentally and theoretically and are well understood nowadays. If the solutions at hand contain chemicals that react such that this reaction changes the density or viscosity *in situ*, an interplay between reactions and hydrodynamics can come into play (De Wit et al. (2012), De Wit (2016)). We will describe here the major influence that reactions can have on such instabilities. In particular, we will explain how, by changing the physical property controlling the hydrodynamic flow, reactions can be used to control the location and amplitude of the convective motions. As a corollar, flows can also be used to tune the yield and spatio-temporal distribution of the chemicals. This control over the pattern formation in reactive fluids sets up the basis of chemo-hydrodynamic pattern selection at the heart of this review.

Of course, the subject is very vast and flows of reactive fluids are encountered in numerous applications ranging from convective motions in stars or in planet interiors, atmospheric chemistry, engineering applications like combustion, blooming of bacteria in oceanic currents and many more. We will necessarily have to make a choice. Dictated by our own research in the field, we will focus here mainly on reactive interfaces in porous media flows but will, as much as possible, point towards the generality of the chemo-hydrodynamic control described. To do so, we will first introduce the mobility profile that is at the heart of the viscously and buoyancy-driven instabilities we will discuss and the influence of chemical reactions on them. Next, we will describe briefly the properties of the hydrodynamic viscous fingering, Rayleigh-Taylor and double-diffusive instabilities in absence of any reaction to be able to appreciate in a second part the effect of reactions on their dynamics.

2. REACTIVE INTERFACE IN A POROUS MEDIUM

Without any loss of generality, we will consider here an interface between two semi-infinite regions in a homogeneous porous medium with constant permeability κ. In this system, a solution of reactant A with initial concentration a_o is put in contact along a contact line at initial time with a solution of another reactant B with initial concentration b_o. The two solutions are both considered diluted and to have their own viscosity μ and density ρ. In absence of any flow, the two reactants meet by diffusion and a simple chemical reaction

$$A + B \rightarrow C \tag{1}$$

takes place in the mixing zone, generating the product C. We seek to understand how this reactive two-layer stratification can be destabilized by viscosity or density gradients and how the reaction can modify the properties of the hydrodynamic instability. For incompressible flows, the dynamics in porous media can be described by the following system of reaction-diffusion-convection (RDC) equations :

$$\underline{\nabla}.\underline{u} = 0, \tag{2}$$

$$\underline{\nabla} p = -\frac{\mu}{\kappa}\underline{u} + \rho \underline{g}, \tag{3}$$

$$\frac{\partial a}{\partial t} + \underline{u}.\underline{\nabla} a = D_A \nabla^2 a - kab, \tag{4}$$

$$\frac{\partial b}{\partial t} + \underline{u}.\underline{\nabla} b = D_B \nabla^2 b - kab, \tag{5}$$

$$\frac{\partial c}{\partial t} + \underline{u}.\underline{\nabla} c = D_C \nabla^2 c + kab, \tag{6}$$

where a, b and c denote respectively the concentrations of the two reactants A, B and of the product C, k is the kinetic constant, p is the pressure, $\underline{u}$ is the velocity field while $D_{A,B,C}$ are the diffusion coefficients of the species A, B and C respectively. Eq.(3) is Darcy's law relating the velocity field $\underline{u}$ to the gradient of pressure. The interplay between reactions and hydrodynamics arises thanks to the dependence of either viscosity μ, density ρ or permeability κ on the concentrations. The model equations (2-6) need therefore to be complemented in each case by a state equation expressing this dependence, in addition to given initial and boundary conditions for all variables. This state equation will depend on the instability considered but common features can be sketched in terms of the relevant mobility profile.

3. MOBILITY PROFILE

The essence of the chemical control of convective motions lies in the control of the mobility profile at the origin of the hydrodynamic instability. The mobility profile $M(x)$ is here defined as the function describing the way the physical property M, which is the motor of the instability, varies along a given spatial coordinate x (Homsy (1987), Manickam & Homsy (1995)). It is a direct consequence of the state equation. In the cases to be analyzed here, M is typically the viscosity μ, the density ρ or the permeability κ. **Figure 1** shows various profiles $M(x)$ that van develop in miscible systems when two different fluids or two solutions of a same solvent but different chemical composition are put in contact. As they usually have different densities or viscosities, there is a jump in this property across

the initial contact line. Upon diffusive mixing, M typically expands as an error function. **Figures 1a,b** show two examples of such profiles at a given time after contact. Depending on the arbitrary choice of orientation of the x axis, M is then either decreasing (**Figure 1a**) or increasing (**Figure 1b**) along x. As will be shown later, the typical influence of reactions or of the presence of chemicals with different diffusion coefficients is to modify these reference mobility profiles either by changing the gradient of M or by introducing extrema in M (**Figures 1c-f**). We will review below how reactions can induce these changes in the mobility profile and what are their consequences on the dynamics. Before doing so, let us first review the hydrodynamic instabilities that can develop in presence of a monotonic mobility profile like those of **Figure 1a,b**.

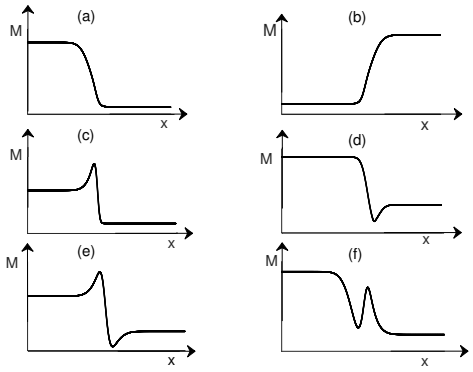

Figure 1: Mobility profiles $M(x)$ giving the spatial dependence of a given physical property of the fluid like its viscosity or density as a function of space. (a) Monotonic decreasing along x; (b) Monotonic increasing along x; (c) Non-monotonic with a maximum; (d) Non-monotonic with a minimum; (e) Non-monotonic with two extrema with amplitude larger than the two end-points values of M; (f) Non-monotonic with two extrema with amplitude smaller than the two end-points values of M.

4. HYDRODYNAMIC INSTABILITIES

4.1. Viscous fingering

When a less viscous fluid displaces a more viscous one in a porous medium, the interface between the two is unstable towards viscous fingering inducing a fingered deformation of the miscible mixing zone (Saffman & Taylor (1958), Homsy (1987)). In that case, the typical unstable mobility profile is the one of viscosity such as in **Figure 1b** where the mobility M is the dynamic viscosity μ and x is the direction of injection. The reverse monotonic decreasing viscosity profile corresponding to a more viscous fluid displacing along x a les viscous one (as in **Figure 1a**) is on the contrary stable.

4.2. Buoyancy-driven instabilities

When the mobility profile M is giving the spatial dependence of the density ρ, various instabilities can develop depending on the orientation of the interface between two different

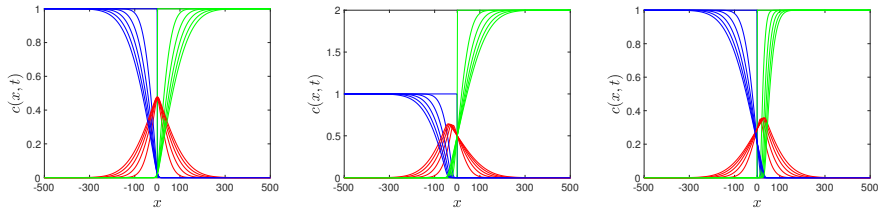

Figure 2: One-dimensional RD concentration profiles of A (blue), B (green) and C (red) for (a) equal diffusion coefficients and initial concentrations, (b) equal diffusion coefficients but larger concentration of B and (c) same initial concentrations but A diffuses 5 times faster than B shown at successive times. x_o is the position of the front at $t = 0$.

fluids A and B with regard to the gravity field and on the diffusivities of the species involved. To connect to reactive solutions later, let us consider that, initially a solution of species A is put in contact along a line with a miscible solution of B. Both species contribute to change the density of the solution. If initially, the interface between the two miscible solutions is vertical, the mobility profiles where $M = \rho$ here are those of **Figures 1a,b** with x pointing perpendicularly to the gravity field. The stratification always gives convection as the denser solution sinks below the other one, inducing a gravity current (Meiburg & Kneller (2010)).

A Rayleigh-Taylor (RT) instability develops across an initially horizontal interface when a denser fluid lies above a less dense one in the gravity field. If x points downwards along the gravity field, then the unstable density profile in the non reactive case is the one of **Figure 1a** with $M = \rho$. Regular fingers develop then symmetrically across the interface (Wooding (1969), Fernandez et al. (2002)). However, even in the case of a stratification of less dense fluid on top of a denser one like in **Figure 1b**, an instability can develop due to double-diffusion (Turner (1979), Radko (2013)). If the lower solute B diffuses faster than the upper solute A, then a double-diffusive (DD) instability destabilizes the interface into density fingering similar to the one of the RT modes while a diffusive layer convection (DLC) mode giving disconnected localized convective zones both above and below the interface is obtained when the upper A diffuses faster than the lower B (Trevelyan et al. (2011), Carballido-Landeira et al. (2013)). In miscible solutions containing two different solutes A and B with different diffusivities, the RT and double-diffusive modes can interact giving rise for instance to specific mixed modes fingers where the difference in diffusion of the species deform the tip of the RT fingers into antennas (Carballido-Landeira et al. (2013)). Similarly, double diffusive effects can control the onset times and intensity of the convective velocity of RT modes (Gopalakrishnan et al. (2018)). All these effects will be at play in reactive systems where different solutes with different diffusion coefficients are involved in the reactions.

To appreciate the effect of simple bimolecular reactions on hydrodynamics, it is important to first understand the properties of reaction-diffusion fronts as their concentration profiles control the mobility profile at the heart of the hydrodynamics.

5. REACTION-DIFFUSION $A + B \to C$ CHEMICAL FRONTS

The properties of $A + B \to C$ reaction-diffusion (RD) fronts where the reactant solutions of A and B in respective concentrations a_o and b_o, are put in contact at $t = 0$ at a location

$x = x_0$ and react according to a bimolecular A+B→C kinetics, have been thoroughly studied since the pioneering work of Gálfi & Rácz (1988). When A and B meet by diffusion, they react producing C in the miscible contact zone. Depending on the relative value of the diffusion coefficients D_A and D_B of reactants A and B and on the ratio $\beta = b_o/a_o$ of their initial concentrations, the front can move in either directions. The reaction front position defined as the location where $\mathcal{R}$ is maximum stays at $x = 0$ if A and B have the same diffusion coefficient and $\beta = 1$ as shown on **Figure 2a**. This is related to the fact that the diffusive flux of A towards the reaction front is then the same as the flux of B. If however $a_0^2 D_A \neq b_0^2 D_B$, these two fluxes differ and the front moves towards the region which has the smallest diffusive flux (Gálfi & Rácz (1988), Jiang & Ebner (1990), Gérard & De Wit (2009)). As an example, for equal diffusion coefficients, the more concentrated solution invades the other one (**Figure 2b**). On the other hand, when $\beta = 1$, the front invades the reactant of lowest diffusion coefficient (**Figure 2c**). We see thus that, depending on the initial concentrations and nature (and more specifically diffusion coefficient) of the reactants, the RD concentration profiles of reactants A and B and of the product C can evolve symmetrically (**Figure 2a**) with regard to the initial position of the front or, on the contrary, develop asymmetries (**Figure 2b,c**). This will, in turn affect the related mobility profiles if the chemical species have an active effect on density or viscosity. Note that, in flow conditions such that the reactants are passively advected, the properties of the RD fronts are recovered in a rectilinear geometry while, in radial geometries, the properties of the front can be tuned by varying the flow rate (Brau et al. (2017), Trevelyan & Walker (2018)). Let us now review what happens if the chemical species are actively changing the flow, starting with the effect on viscosity before addressing the changes in density.

6. HYDRODYNAMIC INSTABILITIES IN REACTIVE FLUIDS

6.1. Viscous fingering in reactive systems

In absence of any reaction, viscous fingering (VF) develops when a less viscous fluid displaces a more viscous one in a porous medium. This instability has been thoroughly studied both experimentally and theoretically because, among others, of its ubiquity in oil recovery when a fluid like water or CO_2 displaces the more viscous oil in the soils (Saffman & Taylor (1958), Homsy (1987)). In this context, reactions producing for instance surfactants *in situ* can modify the local surface tension and affect the Safmann-Taylor instability between two immiscible fluids (Jahoda & Hornof (2000), Nasr-El-Din et al. (1990), Hornof & Baig (1995), Fernandez & Homsy (2003), Niroobakhsh et al. (2017), Tsuzuki et al. (2019)). We won't review this particular case as we focus here on miscible systems. VF is also observed in chromatography, a separation technique by which a mixture of chemical components dissolved in a given solvent is separated via dispersion at different speeds in a porous matrix and/or selective adsorption on the solid phase (Guiochon et al. (2006)). If the carrier fluid has a different viscosity than the sample solvent, VF can appear, which is dramatic for the efficiency of separation (Dickson et al. (1997), Broyles et al. (1998), De Wit et al. (2005), Rousseaux et al. (2007, 2011)). In this context, it has been shown that adsorption on the porous matrix of components controling the viscosity of the fluids can influence the instability (Mishra et al. (2007), Rana et al. (2014, 2018)). As an example, the onset time of the instability can, in some cases, depend nonmonotonically on the retention parameter of the solute adsorption (Hota et al. (2015)).

Note that several works have analyzed VF of miscible autocatalytic fronts able to form

a self-organized interface between the reactants and products of an autocatalytic front (De Wit & Homsy (1999b,a), Swernath & Pushpavanam (2007, 2008), Ghesmat & Azaiez (2009)). The reactions can modify the relative stability of the front and induce the formation of isolated droplets if the reaction is bistable.

The interplay of chemistry and VF occurs through the influence of reactions on viscosity. As, in Darcy's law, the effect on mobility for viscous fingering comes into the mobility ratio $M = \kappa/\mu$ via changes in viscosity, it is logical that changes in the permeability κ via dissolution or precipitation reactions affecting the pore space of the porous matrix will also be able to trigger fingering. This has long been known in studies on infiltration instabilities, where the invading fluid reacts with the solid matrix leading to dissolution of the solid phase and an increase in porosity (Chadam et al. (1986), Daccord & Lenormand (1987), Szymczak & Ladd (2014)). More recent works have shown that precipitation locally decreasing the permeability can also induce fingering (Nagatsu et al. (2014)) leading to beautiful precipitation patterns in various contexts including chemical gardens (Haudin et al. (2014)) or CO_2 mineralization reactions (White & Ward (2012), Schuszter et al. (2014)). With no surprise, concomitant changes in viscosity and permeability can induce an interplay between viscous and precipitation-driven fingering giving rise to interesting new patterns (Nagatsu et al. (2008a), Haudin & De Wit (2015)).

Let us here explain in more details the analytical and numerical developments showing how simple A+B→C reactions can influence or even trigger VF before explaining how these theoretical predictions allow to rationalize the various experimental observations made.

6.2. Viscous fingering of $A + B \rightarrow C$ chemical fronts

6.2.1. Viscosity profiles in reactive systems. If all three species A, B and C influence the viscosity, we have in the most general case that $\mu(\underline{r}, t) = \mu(a, b, c)$ i.e. the viscosity profile depends on the concentration profiles $a(\underline{r}, t), b(\underline{r}, t), c(\underline{r}, t)$ of both reactants A, B and product C. This state equation couples the RDC equations for the concentrations to the flow equation. The viscosities $\mu_A = \mu(a_0, 0, 0), \mu_B = \mu(0, a_0, 0)$ and $\mu_C = \mu(0, 0, a_0)$ represent the viscosity of the fluid when only one of the chemical species is present in concentration a_0. For simplicity, theoretical studies usually assume an exponential relation

$$\mu = \mu_A \; e^{(R_b b + R_c c)/a_0} \tag{7}$$

where R_b and R_c are the log mobility ratios defined as

$$R_b = ln\left[\frac{\mu_B}{\mu_A}\right] \quad \text{and} \quad R_c = ln\left[\frac{\mu_C}{\mu_A}\right]. \tag{8}$$

The parameter R_b compares the viscosity of the two reactant solutions while R_c measures the ratio between the viscosities of the product C and reactant A solutions. In absence of any reaction and if A is injected into B, VF takes places when $R_b > 0$ i.e. if the displacing solution of A is less viscous than the displaced solution of B.

In the reactive case, as soon as the reactants A and B come into contact via diffusion, the chemical reaction is triggered generating the product C in the reactive zone (Hejazi et al. (2010)). The changes in the concentrations profiles reshape the viscosity profiles which can, depending on the relative values of R_b and R_c, become non-monotonic with a maximum if C is sufficiently more viscous than the reactants or with a minimum if C is, on the contrary, decreasing the viscosity (**Figure 3**).

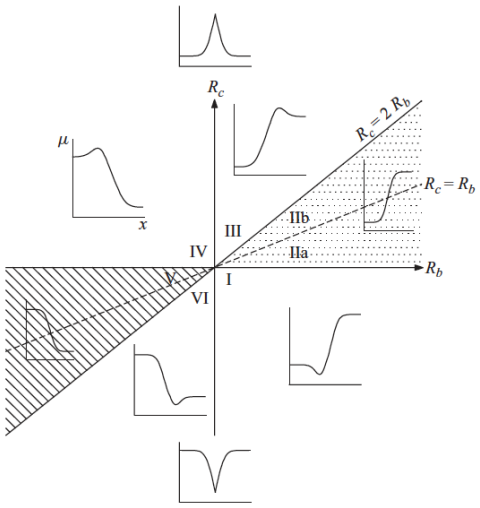

Figure 3: Viscosity profiles depending on the relative values of the log-mobility ratios R_b and R_c. From ref.(Hejazi et al. (2010)).

6.2.2. Theoretical studies. Linear stability analysis (LSA) of these viscosity profiles modified by reactions have discussed two different cases depending whether the reference non reactive situation is unstable or not. If the underlying non reactive system is already unstable because a less viscous solution of A displaces a more viscous solution of B ($R_b > 0$, **Figure 1b**), the reaction modifies the stability properties because, unless $R_c = R_b$ which is the equivalent of the non-reactive case, the presence of the product C modifies the viscosity profile (Hejazi et al. (2010)). The LSA predicts that the reactive situations are always more unstable than their nonreactive counterpart for relatively large time because the gradient of viscosity is steepened by the reaction either in the frontal part of the reaction zone where C pushes B when $R_c < R_b$ or in the rear part of the reaction zone where A pushes C when $R_c > R_b$. Strikingly, the LSA also shows that injecting a more viscous fluid into a less viscous fluid ($R_b < 0$), a situation classically stable in non reactive systems, can also induce instabilities when the reaction induces non-monotonic viscosity profiles (Hejazi et al. (2010)). Fingering then develops thanks to the local region where the viscosity increases along the displacement direction. This means that, for a non-monotonic profile with a maximum, fingering develops at the back of the extremum while in presence of a minimum, fingering is expected in the frontal part of the extremum.

Nonlinear simulations confirm the predictions of the LSA, in the sense that the reactive cases for $R_b > 0$ are all more unstable than the non reactive situation, with fingering starting earlier and with a smaller wavelength. Different morphologies of fingers are also observed : fingers become thinner and their center of mass is more and more displaced towards the back when R_c is increased above R_b (**Figure 4**, bottom) (Nagatsu & De Wit (2011), Hejazi & Azaiez (2010b)). In case of a maximum in viscosity, fingers develop backwards in the zone where A pushes the more viscous C while the frontal part where the more viscous C invades the less viscous B is stable. On the contrary, if R_c is sufficiently lower than R_b such that a minimum in viscosity builds up, more active forward fingering is observed where less viscous C pushes B while the rear part is stabilized. More efficient coarsening decreases

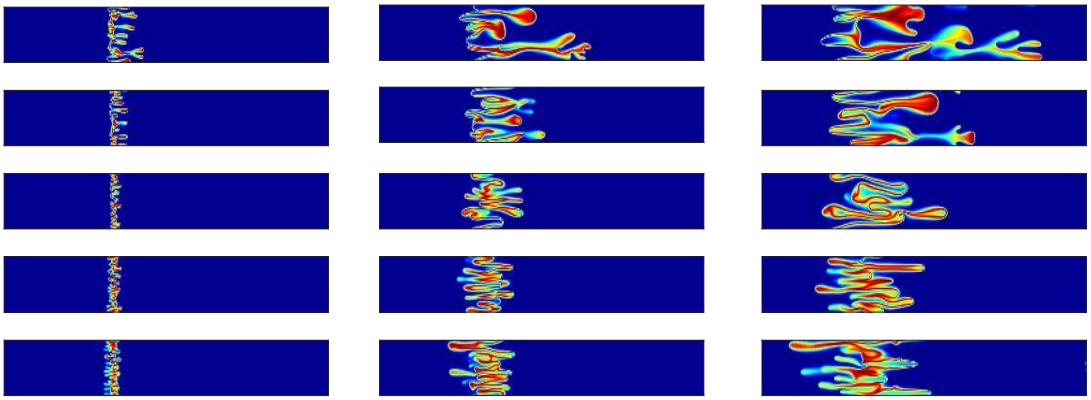

Figure 4: Numerical concentration profiles of C at three successive times from left to right showing VF with $R_b = 2$ modified by reactions for $R_c = -2; 0; 2; 4; 6$ from top to bottom.

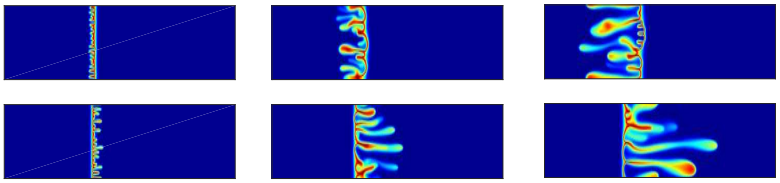

Figure 5: Numerical concentration profiles of C at three successive times from left to right showing reaction-driven VF for $R_b = -1$ triggered by a maximum for $R_c = 4$ (a) or a minimum for $R_c = -6$ (b) in viscosity when a more viscous solution of A displaces a less viscous solution of B.

the number of fingers while tip splitting events are more often observed (**Figure 4**, top) (Nagatsu & De Wit (2011), Hejazi & Azaiez (2010b)). Note that even if the viscosity ratio of the displaced and displacing solutions in the unfavorable part of the profile is the same, the situation with a minimum leads to a faster progression of the fingers at the frontal part with a larger mixing zone than for the reverse fingers associated to a maximum in viscosity because the fingers then develop along the flow rather than against it (Mishra et al. (2010a)).

When $R_b < 0$, the non reactive case is stable. Yet, reactions can then trigger fingering when a non-monotonic viscosity profile builds up. In presence of a minimum, forward fingering is observed where the less viscous C pushes B (**Figure 5**b). In case of a maximum, the unfavorable viscosity jump is located in the trailing zone where A displaces the more viscous C and reverse fingering is favored (**Figure 5**a). This shows thus that reactions are able to destabilize an otherwise hydrodynamically stable situation (Riolfo et al. (2012)). The case of reversible reactions has also been tackled, showing that, depending on the viscosities of the reactant and product solutions, reversibility may enhance/attenuate the instability (Alhumade & Azaiez (2013)).

Nonlinear simulations have also analysed the effect of A+B→C reactions in the case of

a finite size sample of B displaced in a rectilinear geometry within a fluid A. Both interfaces where A pushes B and B pushes A are then present in the same system (Gérard & De Wit (2009), Hejazi & Azaiez (2010a)). Such studies also allow to analyze the possible interaction between the two different interfaces and discuss the influence of reactivity on the spreading due to VF of finite size pollutant zones. Even if the reactant solutions have the same viscosity ($R_b = 0$), such fronts can feature different fingering dynamics when the product C is more viscous and the diffusion coefficients or initial concentrations of the two reactants are different (Gérard & De Wit (2009)). Indeed, because of the asymmetry of the C profile that differential diffusion or concentrations induce (as seen on **Figure 2**), the non-monotonic viscosity profile is also asymmetric with different unfavorable viscosity gradients depending whether A or B is the displacing solution. This evidences the possible fine tuning of the chemical control of local fingering dynamics via the right selection of chemical species with specific differences in concentration or diffusion coefficients. With variable diffusivities, double diffusion effects can, in addition, also come into play (Mishra et al. (2010b)).

Note that control of the viscosity profile via extrema to obtain stabilization of fingering or on the contrary destabilization of an otherwise stable displacement can be further tuned via the addition of nanocatalysts acting on the reaction rate (Ghesmat et al. (2013), Sabet et al. (2017, 2018), Dastvareh & Azaiez (2019)), or the local production of foams (Kahrobaei et al. (2017)) which enlarges the range of action. Interestingly, the geometry also matters as it has been shown that, in a radial injection, the fact that the local speed decreases with the radius from injection influences the production of C (Brau et al. (2017), Trevelyan & Walker (2018)) and thus changes the fingering of finite size samples (Sharma et al. (2019)). In the case where the reactants and the chemical product all have different viscosities, the wealth of possible different dynamics of course increases (Hejazi & Azaiez (2010a)).

6.2.3. Experimental results. Experiments demonstrating the influence of chemical reactions on the properties of miscible viscous fingering are typically conducted in Hele-Shaw cells consisting in 2 glass or plexyglas plates separated by a thin gap in which a host solution of a reactant B is contained (Nagatsu (2015)). Another reactant A is then injected radially or rectilinearly into the cell at a constant flow rate and the A+B→C reaction can proceed in the miscible contact zone between them. If the reaction does not change the viscosity *in situ*, the chemical species are then simply slaved to the flow and the concentration pattern depends on the initial concentrations and injection flow rate (Nagatsu (2015), Nagatsu & Ueda (2001, 2003, 2004)).

The first experiments on reactive VF where an A+B→C type of reaction is actively changing the viscosity and hence affects VF have been performed by Nagatsu et al. (2007). In these experiments, viscous solutions of polymers, the viscosity of which varies with pH, are displaced by less viscous miscible solutions of various reactants. They observe that the fingering pattern is changed by the reaction. If the reaction is very fast, an increase in viscosity induces wider fingers and a suppression of the shielding effect giving a pattern covering a larger area of the displaced solution. On the contrary, a decrease in viscosity leads to thinner fingers with a stronger shielding effect (Nagatsu et al. (2007, 2010)). This is in good agreement with nonlinear simulations performed for fast reactions (Nagatsu & De Wit (2011), Hejazi & Azaiez (2010b)). Interestingly, for slower reactions, the opposite effect is obtained i.e. respectively wider and thinner fingers for a decrease (Nagatsu et al. (2009)) and increase of viscosity (Nagatsu et al. (2011)). This can be rationalized by a careful

inspection of the relative times of reactions and of advection at the tip or base of the fingers (Nagatsu (2015)). In some cases, the polymer used can exhibit non-newtonian properties. An estonishing growth of fingers in a spiral way has then been observed (Nagatsu et al. (2008b)). All these results showing how the reaction changes the VF pattern have been obtained by Nagatsu et al. in cases where the less viscous aqueous solution of reactants displaces a more viscous polymeric situation but the mobility profile remains monotonic. The non-reactive reference situation is thus already unstable and reactions change here the gradients of viscosities, favouring or slowing down fingering without however producing any local extremum in viscosity (zones IIa and IIb of **Figure 3**).

The case of reactions inducing a non-monotonic increasing viscosity profile with a maximum (zone III of **Figure 3**) has been recently studied in Hele-Shaw cells in the case of a step-growth cross-linking polymerization reaction (Bunton et al. (2017), Stewart et al. (2018)). In absence of reaction, the invading solution is less viscous than the displaced one and VF is obtained. By addition of a reaction initiator in the displacing solution in variable concentration, the amount of the more viscous polymer product can be tuned in the contact zone. The cross-linked reaction product is more viscous which results in a non-monotonic viscosity profile at the interface, affecting flow stability. In particular, the numerically predicted fact that fingers extend preferentially at the back of the reaction zone where the less viscous injected reactant displaces the locally produced more viscous product while the frontal part of the reaction zone is stabilized is recovered in the experiments (Bunton et al. (2017)).

The most striking influence of reactions is however to be able to destabilize an otherwise hydrodynamically stable displacement, i.e. typically when the displacing solution is more viscous or of same viscosity than the displaced solution ($R_b \leq 0$). In absence of reactions, the interface is stable and no fingering can develop. As shown theoretically, extrema in the viscosity profile can however destabilize the displacement. Experimentally, Podgorski et al. have for the first time demonstrated chemically-driven VF when the reaction forms a more viscous elastic micellar product following contact between two reactants solutions of the same viscosity (Podgorski et al. (2007)) (axis $R_c > 0$ for $R_b = 0$). The fingering patterns are different depending whether A is injected into B or vice versa, which can be related to the asymmetry of the underlying viscosity profiles (Gérard & De Wit (2009)). Purely reaction-driven fingering has also been obtained when a viscous polymer reaction displaces a less viscous reactant solution and a maximum (zone IV of **Figure 3**) or minimum (zone VI of **Figure 3**) in viscosity is produced (Riolfo et al. (2012)). As predicted theoretically (Hejazi et al. (2010), Nagatsu & De Wit (2011), Hejazi & Azaiez (2010b)), fingers are then seen in experiments to extend backwards in case of a maximum while they progress ahead of the extremum in case of a minimum (**Figure 6**).

In 3D opaque porous media, reactive fingering has also been analyzed using magnetic resonance. Using the same micelle producing reaction as Podgorski et al. (2007), Rose and Britton have evidenced for the first time in 3D how the *in situ* production of the more viscous product can destabilize the displacement of reactants solutions of similar viscosity in a packed bed filled with borosilicate glass beads (Rose & Britton (2013)).

We have here reviewed how changes in the mobility profile induced by an A+B→C reaction changing locally the viscosity can influence viscous fingering and even trigger fingering in otherwise stable non reactive situations. Note that recent progresses have also studied the interplay of fingering with more complex reactions like nonlinear clock reactions (Escala et al. (2019)) able to trigger sudden large changes of viscosity (Escala et al. (2017)). This is

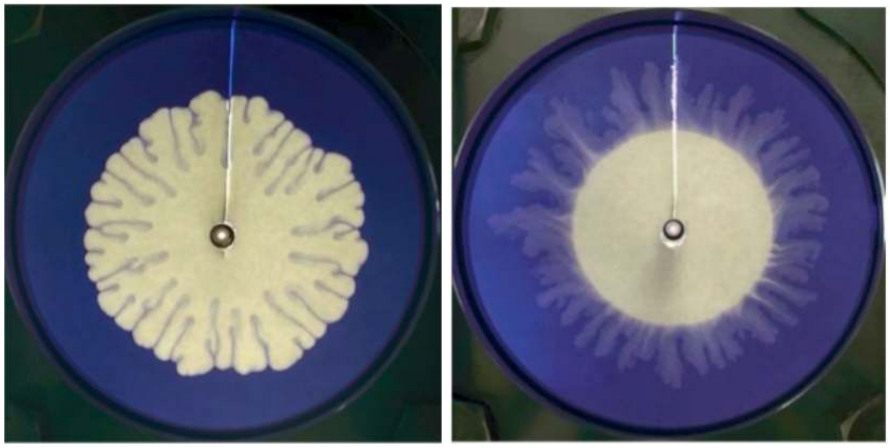

Figure 6: Experimental evidence of reaction-driven viscous fingering in case of a more viscous white solution of polymer displacing a less viscous solution of reactant colored in blue, and such that the reaction induces (a) a local maximum favoring backward fingering; (b) a local minimum inducing forward fingering (Riolfo et al. (2012))

a first step towards using the power of nonlinear oscillating reactions to induce more complex spatio-temporal fingering including oscillating viscous fingers (Rana & De Wit (2019)). Let us now review reactive convection that can be obtained when the mobility profile is related to changes in density.

6.3. Buoyancy-driven instabilities in reactive systems

The density of a given solution is a function of temperature and composition. Let us neglect any heat effect to focus here on compositional effects only. Of course some reactions can be exo- or endothermic and change thus both composition and temperature (Tanoue et al. (2009a,b)) but we will nevertheless neglect heat effect as they have been shown to be negligible in the experiments to be described (Almarcha et al. (2013)). When two solutions, each containing a reactive species, are put in contact in the gravity field, local variations in the density due to the reaction can induce convective motion and mixing.

If all three species A, B and C contribute to changes in density, the coupling between the RDC equations for the concentrations and the flow equation comes from the state equation $\rho(\underline{r},t) = \rho(a,b,c)$. If the solutions are diluted enough, the density is assumed to vary linearly with concentrations as:

$$\rho = \rho_0(1 + \alpha_A a + \alpha_B b + \alpha_C c) \tag{9}$$

where $\alpha_i = (\partial\rho/\partial c_i)/\rho_0$ is the solutal expansion coefficient of species i and c_i its concentration. In dimensionless forms, the important parameters of the problem are the Rayleigh numbers $R_{A,B,C}$ of the reactants A, B and product C respectively, expressing the contribution of each species to the dimensionless density

$$\bar{\rho} = R_A\bar{a} + R_B\bar{b} + R_C\bar{c} \tag{10}$$

where the bar denotes a dimensionless variable. In a porous medium with permeability κ,

the Rayleigh numbers can be defined as

$$R_i = \frac{\alpha_i a_0 \kappa l_c}{\nu D_A} \tag{11}$$

if concentrations are scaled by the initial concentration a_0 of species A and where l_c is the characteristic length of the problem and ν the kinematic viscosity of the solvent. A large variety of different density profiles can then develop depending on the boundary conditions, concentrations and diffusion coefficients of the chemical species (Citri et al. (1990)).

First, if the initial contact line between the two solutions is vertical, the front can be influenced by buoyancy-driven convection as soon as the densities of the species are different (Rongy et al. (2008, 2010), Eckert et al. (2012), Tiani et al. (2018)). Depending on the structure of the density profile, one or two convective rolls can deform the front and induce its propagation (Rongy et al. (2008)). In particular, one convection roll is obtained in case of a monotonic density profile like in **Figures 1a,b** while two counter-rotating vortices are obtained with non-monotonic profiles like those of **Figures 1c,d**. Here again the mobility profile is the key quantity allowing to predict most of the system's behavior. Similar considerations can be discussed in case of gradients of surface tension inducing Marangoni effects if the upper phase is in contact with air (see Tiani et al. (2018) for a review).

In the case of a horizontal contact line between solutions of A and B, buoyancy-driven instabilities influenced or triggered by simple A+B→C reactions can be divided in three main categories depending whether the solutions of A and B are miscible, partially miscible or immiscible. Let us review each category successively.

6.4. Density fingering of miscible A+B→C fronts

In absence of reaction, the stratification of a solution of A above a miscible solution of B develops a Rayleigh-Taylor (RT) instability when the upper layer is denser than the lower one. If the initial stratification is initially statically stable (less dense A above denser B), a double diffusive (DD) instability occurs if B diffuses faster than A while a diffusive layer convection (DLC) mode can be observed if A diffuses faster (Trevelyan et al. (2011)).

In reactive systems, we recover the same instabilities when comparing the relative density and diffusivity of the reactant solutions of A and B. However, the fact that the product C with different density and diffusivity is generated *in situ* can drastically change the situation. **Figure 7** compares experimental patterns that have been obtained in Hele-Shaw cells when putting two miscible solutions of different density in contact along a horizontal line in the gravity field. Note that color indicators can play an active role in the dynamics and change the overall look of the patterns (Almarcha et al. (2010b), Kuster et al. (2011), Mosheva & Shmyrov (2017)), hence **Figure 7** has been obtained using a Schlieren technique tracking changes in index of refraction without any use of color indicator. The upper line features mixing between non reactive solutions of salt and sugar (Carballido-Landeira et al. (2013), Gopalakrishnan et al. (2018)) while the lower line shows the effect of an A+B→C neutralisation reaction on the stratification between aqueous solutions of a strong acid and of a strong base (Tanoue et al. (2009a,b), Zalts et al. (2008), Almarcha et al. (2010a, 2011), Lemaigre et al. (2013), Bratsun et al. (2015)). When the upper solution is denser than the lower one, then the initial condition develops a RT instability (**Figure 7a**) with fingers extending in the non reactive case on average the same distance above and below the initial contact line. If a reaction takes place, the sinking fingers do not develop because

the downward moving denser A is eaten by the reaction and replaced by a salt of lower density (**Figure 7d**) (Almarcha et al. (2010a), Lemaigre et al. (2013)). Similarly, the local production by reaction of the salt C with different density can break the symmetries of the double diffusive (**Figure 7b,e**) and DLC convective modes (**Figure 7c,f**) (Almarcha et al. (2010a), Lemaigre et al. (2013)). In addition, it is observed that the reactive patterns can feature secondary instabilities in time, once enough production of C can trigger for instance the fingered sinking of denser C in the less dense reactant B (Almarcha et al. (2011)) or when differential diffusion effects between the zone rich in C and the lower layer of B (Lemaigre et al. (2013)) come into play. Importantly, even if the reaction is the same i.e. here if the same acid-base neutralisation reaction takes place, the dynamics is extremely sensitive to the nature of the counter-ions which do not participate in the reaction but have a major role in the density profile and diffusion of the chemicals (Almarcha et al. (2011)). Non ideal effects can influence these dynamics. Indeed, if the solutions are not dilute enough, the diffusion coefficients become a function of concentrations which can trigger extrema in non-monotonic density profiles and induce additional local convection (Bratsun et al. (2015)).

Theoretical linear stability analysis (Kim (2014)), nonlinear simulations (Almarcha et al. (2010a), Lemaigre et al. (2013), Kim (2014)) and a classification of all possible density profiles (Almarcha et al. (2011), Lemaigre et al. (2013), Trevelyan et al. (2015)) in the parameter space of the problem can rationalize these experimental observations that chemical reactions can trigger instabilities in otherwise stable situations but also break the symmetry of convective structures and instabilities. To understand this, **Figure 8** shows a variety of possible density profiles around A+B→C fronts, depending on the relative values of the Rayleigh numbers and diffusion coefficients of the three species. We see that the density profile can feature up to 3 extrema in the reaction zone depending on the values of parameters. These extrema can suppress, trigger and localize convection and act as efficient controller of the flows.

Hejazi an Azaiez have further analyzed numerically the case where the chemical product solution C has both a different density and viscosity than the one of the reactant solutions and a transverse flow is applied parallelly to the initial horizontal interface between the reactants (Hejazi & Azaiez (2012, 2013)). They find that, in presence of the transverse flow, fingers with sharp concentration gradients develop and advance faster downward and that higher chemical production rates are obtained.

Recently, chemo-hydrodynamic patterns involving more complex oscillating reactions have been studied as well. In particular, in the A+B→ oscillator case, separate reactants of an oscillatory reaction are put in contact along a horizontal miscible interface. The oscillations in concentration develop then in the local reaction zone (Escala et al. (2014)). As they induce local changes in density, an interplay between localized concentration waves and buoyancy-driven convection produces truly genuine chemo-hydrodynamic structures that would exist neither in oscillating RD systems nor in pure hydrodynamics. Such studies pave the way towards analysing patterns merging the self-organising structure of chemical and hydrodynamical systems (Budroni & De Wit (2017)).

6.5. Influence of $A + B \rightarrow C$ reactions on convective dissolution

The previous section has described buoyancy-driven convection around miscible $A+B \rightarrow C$ fronts when convection can extend both above and below the initial contact line. An

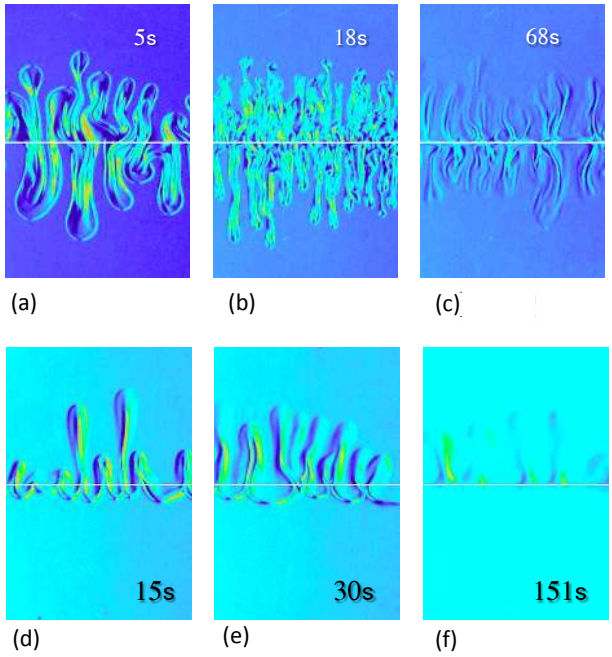

Figure 7: Comparison between experimental non-reactive (upper line) and reactive (lower line) buoyancy-driven patterns in a vertical Hele-Shaw cell due to (a,d) Rayleigh-Taylor, (b,e) double-diffusive and (c,f) diffusive layer convection modes. Field of view: 1.8 cm 2.7 cm. From Lemaigre et al. (2013).

important application of similar dynamics but in partially miscible systems is currently attracting much attention: the case of convective dissolution relevant to CO_2 sequestration, aiming at reducing atmospheric concentrations of this greenhouse gas (Metz et al. (2005)). In this technique, CO_2 is injected into soils, typically in saline aquifers well spread around the globe. After injection, CO_2 rises up to the impermeable cap rock delimitating the aquifer and a two-layer stratification of CO_2 above the salt water is obtained. Upon dissolution of CO_2 in water, a denser boundary layer forms which can become unstable towards buoyancy-driven convection (Riaz et al. (2006), Neufeld et al. (2010), Huppert & Neufeld (2014), Slim (2014), Emami-Meybodi et al. (2015), Thomas et al. (2018)). Depending on the chemical composition of the host aquifer, chemical reactions can take place which affect the density profile and hence convection.

We recover in this application the stratification of a phase A above B with local production of C but the boundary condition is different than the one in the miscible case: the host phase is initially filled only with B and A dissolves into B with a given solubility a_0 from an upper fixed interface. Due to the importance for climate issues of quantifying

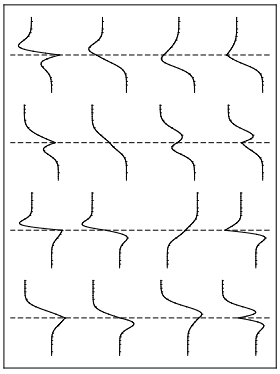

Figure 8: Variety of density profiles that can develop around A+B→ C chemical fronts when all three species have different Rayleigh numbers and diffusion coefficients. The vertical dashed line features the position of the initial contact line between the miscible solutions of A and B. From Trevelyan et al. (2015).

the flux of CO_2 that can dissolve in a given host phase, numerous works have focused on analysing convective dissolution in reactive systems. Let us point here the specificities of this partially miscible case and to what extent reactions can favour convective dissolution.

6.5.1. Theoretical modeling. As said above, the model equations are again Eqs.(2-6) with, as for the miscible case discussed in section 6.4, the density being a function of the concentrations a, b and c. The only differences are in the initial condition ($a = a_0$ at the partially miscible interface and zero in the bulk while $b = b_0$ and $c = 0$ everywhere) and the boundary condition at the interface where zero velocity, no-flux for B, C and $a = a_0$ are applied (Loodts et al. (2016)).

These specific initial and boundary conditions induce a downward progression of buoyancy-driven fingers generated at the interface. There is thus a change of symmetry with regard to the miscible case. Yet, the analysis of density profiles in the partially miscible case helps again to classify all possible dynamics (Loodts et al. (2016)). If all species have the same diffusion coefficients, the important parameters of the problem are the difference $\Delta R_{CB} = R_C - R_B$ between the Rayleigh numbers of the product C and that of the reactant B and the ratio $\beta = b_0/a_0$ between the initial concentration of reactant B and the solubility of A in the host phase.

While simple reactions consuming A out of the solution stabilize convection (Ghesmat et al. (2011), Andres & Cardoso (2011, 2012), Cardoso & Andres (2014), Ward et al. (2014), Kim & Choi (2014), Kim & Kim (2015), Ghoshal et al. (2018)), various theoretical works have shown that A+B→C reactions can accelerate or decelerate the convective dynamics with respect to the nonreactive case and that the steady-state dissolution flux of species A varies with the difference ΔR_{CB} (Loodts et al. (2014, 2015, 2017, 2018), Jotkar et al. (2019), Ghoshal et al. (2017).) For equal diffusion coefficients, if $\Delta R_{CB} > 0$, the density profiles are monotonic. If C is sufficiently denser than B, the density at the interface is increased which gives rise to enhanced convective dissolution, a regime that we refer to as "destabilizing" with regard to the non reactive reference case (**Figure 9**). Conversely, if C

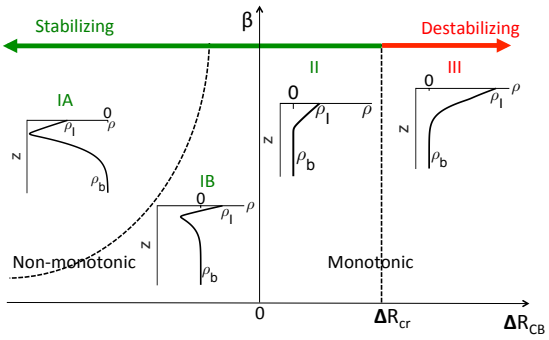

Figure 9: Classification of dimensionless density profiles in the parameter space ($\beta = b_0/a_0$, $\Delta R_{CB} = R_C - R_B$), developing when a species A dissolves at $z = 0$ downwards into a host phase containing a species B and reacts according to the A+B→C scheme to generate the product C (Loodts et al. (2016, 2015), Jotkar et al. (2019)).

is less dense than B ($\Delta R_{CB} < 0$), the density profiles are non-monotonic. The upper part of the profile features density decreasing along gravity which is prone to trigger convection. However, this zone is followed downwards by a stabilizing density barrier that constrains the fingers in a localized zone of space (Loodts et al. (2018), Jotkar et al. (2019), Budroni et al. (2014, 2017)). The resulting nonlinear dynamics can be quite different: in the destabilizing case, long sinking fingers are formed which regularly merge while new fingers appear at the boundary (**Figure 10a**). The activation of the dynamics by chemistry leads to a very active renewed convection as seen on the space-time map of the density along a line just below the interface (**Figure 10b**). In the stabilizing case, the minimum in density freezes the fingers above the extremum at a given fixed wavelength (**Figure 10c**). Only, when the reaction front has traveled a while downward is then merging towards a new larger fixed wavelength obtained (**Figure 10d**). In all reactive cases, the convective flux of A into the host phase is larger than in the non reactive case (Loodts et al. (2017), Jotkar et al. (2019)). The case of reversible reactions and additional viscosity contrasts has also been tackled, showing even more complex scenarios when C can revert to the reactants once formed (Alhumade & Azaiez (2015)). Differential diffusive effects further enlarge the variety of possible dynamics (Loodts et al. (2018), Kim & Cardoso (2018)). Similarly to viscous fingering, buoyancy effects can also be coupled to changes in permeability via dissolution of the porous matrix or precipitation (J. Ennis-King & Paterson (2007), Ritchie & Pritchard (2011), Hidalgo et al. (2015), Binda et al. (2017), Thomas et al. (2019)). Interestingly, reactions are also able to destabilize the otherwise stable case of a species dissolving in a host phase and decreasing its density. In that case, the upper layer is less dense but, if reactions come into play, non-monotonic density profiles can develop triggering local convection (Bees et al. (2001), Loodts et al. (2015, 2016), Kim & Cardoso (2018)).

6.5.2. Experimental results. Convecting dissolution fingering of CO_2 in absence of any reactions has been experimentally evidenced in Hele-Shaw cells using a color indicator tracing

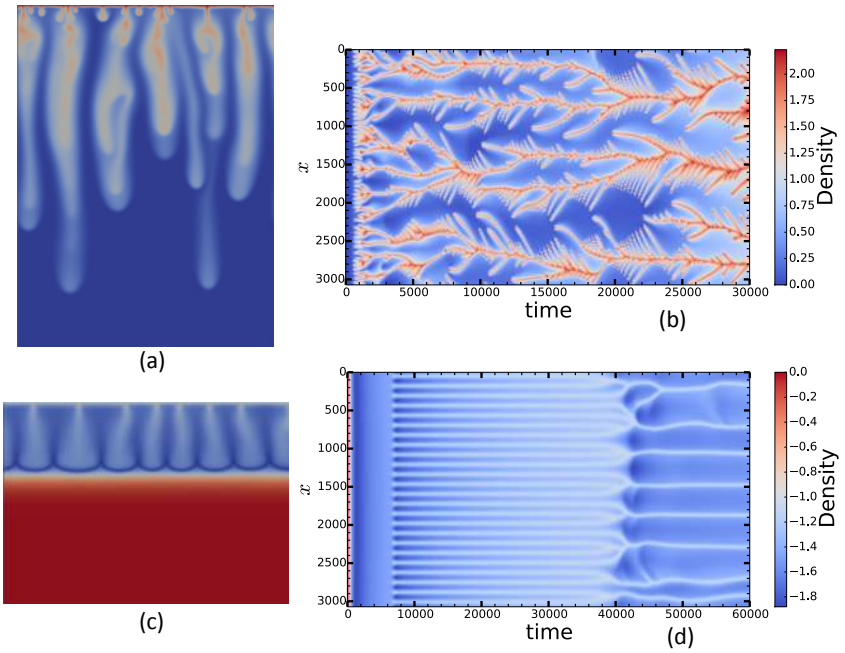

Figure 10: Numerical convective dissolution patterns of density. In the destabilizing case (a), fingers sink downwards rapidly with very active merging and formation of new fingers as seen in the corresponding space-time map (b). In the stabilizing case (c), the non-monotonic density profile with a minimimum is giving a density barrier inducing regular fingers with a constant wavelength in time. As seen on the corresponding space-time map (d), these fingers rearrange after a while to yield a new "frozen" pattern but with a larger wavelength (Loodts et al. (2017), Jotkar et al. (2019)).

the pH decrease within the fingers as CO_2 acidifies the host aqueous phase (Kneafsey & Pruess (2010, 2011)). Outeda et al. (2014) have studied in such systems the temporal evolution of the mixing zone as well as dispersion curves, and the growth rate of the instability for different pressures in CO_2 and different color indicator concentrations. They find that, at earlier time, the growth changes with the concentration of the color indicator and that increasing the pressure destabilizes the system. Using analogous systems, Slim et al. (2013) could quantify the nonlinear dynamics, which is, as seen in simulations, featuring onset of fingering followed by merging and regular formation of new fingers after a while. Here again, color indicators can perturb the dynamics (Thomas et al. (2015)), which is why Schlieren or interferometric optical techniques tracking gradients of index of refraction should be prefered to visualize convection. Experiments confirm that first order reactions where A is consumed while no other species changes the density stabilize the flow (Cardoso

& Andres (2014)). Bimolecular A+B→C reactions where all species participate in density changes can on the contrary either accelerate or decrease convection (Loodts et al. (2014), Budroni et al. (2014, 2017), Wylock et al. (2008, 2011, 2014), Thomas et al. (2015, 2016, 2019), Cherezov & Cardoso (2016)). Strikingly, the acceleration is very sensitive to the nature of all ions present in the host phase which emphasizes the fine tuning that reactions can have on the control of the density profile (Thomas et al. (2016)).

6.6. Effect of A+B→C reactions on buoyancy-driven convection in immiscible systems

Spatio-temporal convective patterns can become quite complex in the case of two immiscible solvents put in contact along a horizontal line, each of them containing a reactant. Upon transfer of one reactant from one phase to the other, a wealth of different convective chemo-hydrodynamic patterns can be observed in both the upper and lower layers (**Figure 11**) (Eckert & Grahn (1999), Eckert et al. (2004), Asad et al. (2010), Schwarzenberger et al. (2012)). The situation is then often complicated by the presence of Marangoni effects due to surface-tension gradients (Bratsun & De Wit (2004)) and modeling needs to account for reaction-diffusion-convection equations in both layers (Bratsun & De Wit (2011)).

7. CONCLUSIONS

Chemical reactions can actively influence or even trigger convective motions when two solutions containing separate reactants are put in contact. We have here reviewed some of their effects on viscous fingering, Rayleigh-Taylor, double diffusive and convective dissolution instabilities. The key in controlling chemically these various hydrodynamic instabilities is in the action that reactions can have on the viscosity or density profiles. Specifically, changes in concentration profiles by the local generation of the product of the reaction after consumption of the reactants and the fact that all species can diffuse at different rates can produce local extrema in the mobility profile that can slow down, favor or generate convection. We have here mainly focused on simple A+B→C reactions but more complex reactions giving spatio-temporal complex reaction-diffusion patterns could also be used, increasing then the power of chemical control. In this regard, development of chemo-hydrodynamic pattern selection aiming at predicting the properties of hydrodynamic instabilities in active reactive systems should seek for new dynamics existing only thanks to the active coupling between reaction-diffusion and convective modes. Note that the control strategy suggested here relies mainly on controlling the mobility profile that is independent of the flow equation. In that respect, studying the various chemo-hydrodynamic instabilities discussed here on Darcy's law in Stokes or Navier-Stokes flows should be an interesting topics for the future.

SUMMARY POINTS

1. Summary point 1. Chemical reactions can influence and even trigger hydrodynamic instabilities by changing the related mobility profile.
2. Summary point 2. Reactions can break the symmetries of convective instabilities and localize the fluid motions.
3. Summary point 3. In viscous fingering, A+B→C reactions can enhance or stabilize fingering when a less viscous reactive solution displaces a more viscous one but can

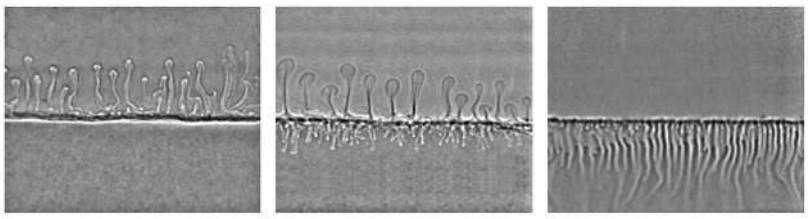

Figure 11: Experimental buoyancy-driven instabilities developing at successive times when an organic upper solvent containing an acid is put in contact with an immiscible lower aqueous solvent containing a base. (a) Initially, downward transfer of the acid creates a depletion zone above the interface inducing upward plumes; (b) Next, the acid and base react close to the interface producing denser sinking fingers of C in the lower layer and thermal plumes in the upper layer; (c) Later, double diffusive effects between the various chemicals diffusing at different rates produce regular fingering in the lower layer. Reproduced with permission from Eckert & Grahn (1999).

also trigger an instability when a more viscous solution is the displacing one by generating a local extremum in viscosity.

4. Summary point 4. For buoyancy-driven flows, bimolecular reactions change the symmetries of Rayleigh-Taylor, double-diffusive and convective dissolution patterns and can induce secondary instabilities in time.
5. Summary point 5. In convective dissolution, reactions can stabilize or destabilize convection but in all cases, increase the dissolution flux towards the host phase.

FUTURE ISSUES

1. Future issue 1. More complex reactions like oscillating reactions could produce pulsatile or patterned convective flows merging the self-organizing power of chemistry and hydrodynamics.

2. Future issue 2. A general theory of chemo-hydrodynamic pattern selection should be developed.
3. Future issue 3. Generalization of the chemical control of porous media flows to flows described by Stokes or Navier-Stokes equations can be guided by a classification of the dynamics on the basis of the reference mobility profiles.

DISCLOSURE STATEMENT

The author is not aware of any affiliations, memberships, funding, or financial holdings that might be perceived as affecting the objectivity of this review.

ACKNOWLEDGMENTS

I warmly thank all coauthors and colleagues with whom I have collaborated over the years, in particular G.M. Homsy for numerous inspiring discussions. I thank also C. Rana and M. Jotkar for their help in preparing figures for this manuscript.

LITERATURE CITED

Alhumade H, Azaiez J. 2013. Stability analysis of reversible reactive flow displacements in porous media. *Chem. Eng. Sci* 101:46

Alhumade H, Azaiez J. 2015. Numerical simulations of gravity driven reversible reactive flows in homogeneous porous media. *Math. Probl. Engin.* 2015:920692

Almarcha C, R'Honi Y, De Decker Y, Trevelyan PMJ, Eckert K, De Wit A. 2011. Convective mixing induced by acid-base reactions. *J. Phys. Chem. B* 104:044501

Almarcha C, Trevelyan PMJ, Grosfils P, De Wit A. 2010a. Chemically driven hydrodynamic instabilities. *Phys. Rev. Lett.* 104

Almarcha C, Trevelyan PMJ, Grosfils P, De Wit A. 2013. Thermal effects on the diffusive layer convection instability of an exothermic acid-base reaction front. *Phys. Rev. E* 88:033009

Almarcha C, Trevelyan PMJ, Riolfo L, Zalts A, El Hasi C, et al. 2010b. Active role of a color indicator in buoyancy-driven instabilities of chemical fronts. *J. Phys. Chem. Lett.* 1:752–757

Andres JTH, Cardoso SSS. 2011. Geochemistry of silicate-rich rocks can curtail spreading of carbon dioxide in subsurface aquifers. *Phys. Rev. E* 83:046312

Andres JTH, Cardoso SSS. 2012. Convection and reaction in a diffusive boundary layer in a porous medium: nonlinear dynamics. *Chaos* 22:037113

Asad A, Yang YH, Chai C, Wu J. 2010. Hydrodynamic instabilities driven by acid-base neutralization reaction in immiscible system. *Chinese J. Chem. Phys.* 23:513–520

Bees MA, Pons AJ, Sorensen PG, Sagués F. 2001. Chemoconvection: A chemically driven hydrodynamic instability. *J. Chem. Phys.* 114:1932

Binda L, El Hasi C, Zalts A, D′Onofrio A. 2017. Experimental analysis of density fingering instability modified by precipitation. *Chaos* 27:053111

Bratsun D, De Wit A. 2004. On Marangoni convective patterns driven by an exothermic chemical reaction in two-layer systems. *Phys. Fluids* 16:1082–1096

Bratsun D, De Wit A. 2011. Buoyancy-driven pattern formation in reactive immiscible two-layer systems. *Chem. Eng. Sci.* 66:5723–5734

Bratsun D, Kostarev K, Mizev A, Mosheva E. 2015. Concentration-dependent diffusion instability in reactive miscible fluids. *Phys. Rev. E* 92:011003(R)

Brau F, Schuszter G, De Wit A. 2017. Flow control of A+B→C fronts by radial injection. *Phys. Rev. Lett.* 118:134101

Broyles B, Shalliker R, Cherrak D, Guiochon G. 1998. Visualization of viscous fingering in chromatographic columns. *J. Chromatog. A* 822:173

Budroni MA, De Wit A. 2017. Dissipative structures: From reaction-diffusion to chemo-hydrodynamic patterns. *Chaos: An Interdisciplinary Journal of Nonlinear Science* 27:104617

Budroni MA, Riolfo LA, Lemaigre L, Rossi F, Rustici M, De Wit A. 2014. Chemical control of hydrodynamic instabilities in partially miscible two-layer systems. *J. Phys. Chem. Letters* 5:875–881

Budroni MA, Thomas C, De Wit A. 2017. Chemical control of dissolution-driven convection in partially miscible systems: nonlinear simulations and experiments. *Phys. Chem. Chem. Phys.* 19:7936

Bunton P, Tullier M, Meiburg E, Pojman J. 2017. The effect of a crosslinking chemical reaction on pattern formation in viscous fingering of miscible fluids in a Hele-Shaw cell. *Chaos* 27:104614

Carballido-Landeira J, Trevelyan P, Almarcha C, De Wit A. 2013. Mixed-mode instability of a miscible interface due to coupling between Rayleigh-Taylor and double-diffusive convective modes. *Phys. Fluids* 25:024107

Cardoso SSS, Andres JTH. 2014. Geochemistry of silicate-rich rocks can curtail spreading of carbon dioxide in subsurface aquifers. *Nat. Commun.* 5:5743

Chadam J, Hoff D, Merino E, Ortoleva P, Sen A. 1986. Reactive infiltration instabilities. *IMA J. Appl. Math.* 36:207–221

Cherezov I, Cardoso SSS. 2016. Acceleration of convective dissolution by chemical reaction in a Hele-Shaw cell. *Phys. Chem. Chem. Phys.* 18:23727–23736

Citri O, Kagan M, Kosloff R, Avnir D. 1990. Evolution of chemically induced unstable density gradients near horizontal reactive interfaces. *Langmuir* 6:559–564

Daccord G, Lenormand R. 1987. Fractal patterns from chemical dissolution. *Nature* 325:41–43

Dastvareh B, Azaiez J. 2019. Instabilities of nonisothermal nanocatalytic reactive flows in porous media. *Phys. Rev. Fluids* 4:034003

De Wit A. 2016. Chemo-hydrodynamic patterns in porous media. *Phil. Trans. Roy. Soc. A* 374:20150419

De Wit A, Bertho Y, Martin M. 2005. Viscous fingering of miscible slices. *Phys. Fluids* 17:054114

De Wit A, Eckert K, Kalliadasis S. 2012. Introduction to the focus issue: Chemo-hydrodynamic patterns and instabilities. *Chaos* 22:037101

De Wit A, Homsy GM. 1999a. Nonlinear interactions of chemical reactions and viscous fingering in porous media. *Phys. Fluids* 11:949–951

De Wit A, Homsy GM. 1999b. Viscous fingering in reaction-diffusion systems. *Journal of Chemical Physics* 110:8663–8675

Dickson ML, Norton TT, Fernandez EJ. 1997. Chemical imaging of multicomponent viscous fingering in chromatography. *AIChE Journal* 43:409–418

Eckert K, Acker M, Shi Y. 2004. Chemical pattern formation driven be a neutralization reaction. mechanism and basic features. *Phys. Fluids* 16:385–399

Eckert K, Acker M, Tadmouri R, Pimienta V. 2012. Chemo-Marangoni convection driven by an interfacial reaction: Pattern formation and kinetics. *Chaos* 22:037112

Eckert K, Grahn A. 1999. Plume and finger regimes driven by an exothermic interfacial reaction. *Phys. Rev. Lett.* 82:4436

Emami-Meybodi H, Hassanzadeh H, Green CP, Ennis-King J. 2015. Convective dissolution of CO_2 in saline aquifers: Progress in modeling and experiments. *Int. J. Greenhouse Gas Control* 40:238–266

Escala DM, Carballido-Landeira J, De Wit A, Muñuzuri AP. 2014. Self-organized traveling chemo-hydrodynamic fingers triggered by a chemical oscillator. *J. Phys. Chem. Letters* 5:413–418

Escala DM, De Wit A, Carballido-Landeira J, Muñuzuri AP. 2019. Viscous fingering induced by a

pH-sensitive clock reaction. *Langmuir*

Escala DM, Muñuzuri AP, De Wit A, Carballido-Landeira J. 2017. Temporal viscosity modulations driven by a pH sensitive polymer coupled to a pH-changing chemical reaction. *Phys. Chem. Chem. Phys.* 19:11914

Fernandez J, Homsy GM. 2003. Viscous fingering with chemical reaction: effect of in-situ production of surfactants. *Journal of Fluid Mechanics* 480:267–281

Fernandez J, Kurowski P, Petitjeans P, Meiburg E. 2002. Density-driven unstable flows of miscible fluids in a Hele-Shaw cell. *J. Fluid Mech.* 451:239

Gálfi L, Rácz Z. 1988. Properties of the reaction front in an A+B→C type reaction-diffusion process. *Phys. Rev. A* 38:6

Gérard T, De Wit A. 2009. Miscible viscous fingering induced by a simple A+B→C chemical reaction. *Phys. Rev. E* 79:016308

Ghesmat K, Azaiez J. 2009. Miscible displacements of reactive and anisotropic dispersive flows in porous media. *Transp. Porous Med.* 77:489–506

Ghesmat K, Hassanzadeh H, Abedi J. 2011. The impact of geochemistry on convective mixing in a gravitationally unstable diffusive boundary layer in porous media: CO_2 storage in saline aquifers. *J. Fluid Mech.* 673:480–512

Ghesmat K, Hassanzadeh H, Abedi J, Chen Z. 2013. Frontal stability of reactive nanoparticle transport during in situ catalytic upgrading of heavy oil. *Fuel* 107:525–538

Ghoshal P, Kim MC, Cardoso SSS. 2017. Reactive-convective dissolution in a porous medium: the storage of carbon dioxide in saline aquifers. *Phys. Chem. Chem. Phys.* 19:644–655

Ghoshal P, Kim MC, Cardoso SSS. 2018. Onset of convection in the presence of a precipitation reaction in a porous medium: A comparison of linear stability and numerical approaches. *Fluids* 3:1

Gopalakrishnan S, Carballido-Landeira J, Knaepen B, De Wit A. 2018. Control of Rayleigh-Taylor instability onset time and convective velocity by differential diffusion effects. *Phys. Rev. E* 98:011101(R)

Guiochon G, Felinger A, Shirazi DG, Katti AM. 2006. Fundamentals of preparative and nonlinear chromatography. Academic Press

Haudin F, Cartwright JHE, Brau F, De Wit A. 2014. Spiral precipitation patterns in confined chemical gardens. *Proc. Nat. Acad. Sci.* 111:17363–17367

Haudin F, De Wit A. 2015. Patterns due to an interplay between viscous and precipitation-driven fingering. *Physics of Fluids* 27:113101

Hejazi SH, Azaiez J. 2010a. Hydrodynamic instability in the transport of miscible reactive slices through porous media. *Phys. Rev. E* 81:056321

Hejazi SH, Azaiez J. 2010b. Non-linear interactions of dynamic interfaces in porous media. *Chem. Eng. Sci.* 65:938

Hejazi SH, Azaiez J. 2012. Stability of reactive interfaces in saturated porous media under gravity in the presence of transverse flows. *J. Fluid Mech.* 695:439–466

Hejazi SH, Azaiez J. 2013. Nonlinear simulation of transverse flow interactions with chemically driven convective mixing in porous media. *Water Resour. Res.* 49:4607–4618

Hejazi SH, Trevelyan PMJ, Azaiez J, De Wit A. 2010. Viscous fingering of a miscible reactive A+B→C interface: a linear stability analysis. *J. Fluid Mech.* 652:501

Hidalgo JJ, Dentz M, Cabeza Y, Carrera J. 2015. Dissolution patterns and mixing dynamics in unstable reactive flow. *Geophys. Res. Lett.* 42:6357–6364

Homsy GM. 1987. Viscous fingering in porous media. *Ann. Rev. Fluid Mech.* 19:271–311

Hornof V, Baig FU. 1995. Influence of interfacial reaction and mobility ratio on the displacement of oil in a Hele-Shaw cell. *Experiments in Fluids* 18:448–453

Hota T, Pramanik S, Mishra M. 2015. Onset of fingering instability in a finite slice of adsorbed solute. *Phys. Rev. E* 92:023013

Huppert HE, Neufeld JA. 2014. The fluid mechanics of carbon dioxide sequestration. *Ann. Rev.*

Fluid Mech. 46:255–272
J. Ennis-King, Paterson L. 2007. Coupling of geochemical reactions and convective mixing in the long-term geological storage of carbon dioxide. *Int. J. Greenhouse Gas Control* 1:86–93
Jahoda M, Hornof V. 2000. Concentration profiles of reactant in a viscous finger formed during the interfacially reactive immiscible displacements in porous media. *Powder Technology* 110:253–257
Jiang Z, Ebner C. 1990. Simulation study of reaction fronts. *Phys. Rev. A* 42:7483–7486
Jotkar M, De Wit A, Rongy L. 2019. Enhanced convective dissolution due to an A+B→C reaction: control of the non-linear dynamics via solutal density contributions. *Phys. Chem. Chem. Phys.*
Kahrobaei S, Vincent-Bonnieu S, Farajzadeh R. 2017. Experimental study of hysteresis behavior of foam generation in porous media. *Sc. Rep.* 7:8986
Kim M. 2014. Effect of the irreversible A+B→C reaction on the onset and the growth of the buoyancy-driven instability in a porous medium. *Chem. Eng. Sci.* 112:56–71
Kim MC, Cardoso SSS. 2018. Diffusivity ratio effect on the onset of the buoyancy-driven instability of an A+B→C chemical reaction system in a Hele-Shaw cell: Asymptotic and linear stability analyses. *Phys. Fluids* 30:094102
Kim MC, Choi CK. 2014. Effect of first-order chemical reaction on gravitational instability in a porous medium. *Phys. Rev. E* 90:053016
Kim MC, Kim YH. 2015. The effect of chemical reaction on the onset of gravitational instabilities in a fluid saturated within a vertical Hele-Shaw cell: Theoretical and numerical studies. *Chem. Eng. Sci.* 134:632–647
Kneafsey T, Pruess K. 2010. Laboratory flow experiments for visualizing carbon dioxide-induced, density-driven brine convection. *Transp. Por. Med.* 82:123–139
Kneafsey T, Pruess K. 2011. Laboratory experiments and numerical simulation studies of convectively enhanced carbon dioxide dissolution. *Energy Procedia* 4:5114–5121
Kuster S, Riolfo L, Zalts A, El Hasi C, Almarcha C, et al. 2011. Differential diffusion effects on buoyancy-driven instabilities of acid-base fronts: the case of a color indicator. *Phys. Chem. Chem. Phys.* 13:17295–17303
Lemaigre L, Budroni MA, Riolfo LA, Grosfils P, De Wit A. 2013. Asymmetric Rayleigh-Taylor and double-diffusive fingers in reactive systems. *Phys. Fluids* 25:014103
Loodts V, Knaepen B, Rongy L, De Wit A. 2017. Enhanced steady-state dissolution flux in reactive convective dissolution. *Phys. Chem. Chem. Phys.* 19:18565–18579
Loodts V, Rongy L, De Wit A. 2014. Impact of pressure, salt concentration, and temperature on the convective dissolution of carbon dioxide in aqueous solutions. *Chaos* 24:043120
Loodts V, Rongy L, De Wit A. 2015. Chemical control of dissolution-driven convection in partially miscible systems: theoretical classification. *Phys. Chem. Chem. Phys.* 17:29814
Loodts V, Saghou H, Knaepen B, Rongy L, De Wit A. 2018. Differential diffusivity effects in reactive convective dissolution. *Fluids* 3:83
Loodts V, Trevelyan PMJ, Rongy L, De Wit A. 2016. Density profiles around A+B→C reaction-diffusion fronts in partially miscible systems: A general classification. *Phys. Rev. E* 94:043115
Manickam O, Homsy G. 1995. Fingering instabilities in vertical miscible displacement flows in porous media. *J. Fluid Mech.* 288:75–102
Meiburg E, Kneller B. 2010. Turbidity currents and their deposits. *Ann. Rev. Fluid Mech.* 42:135–156
Metz B, Davidson O, de Conninck H, Loos M, Meyer L. 2005. In *Intergovernmental Panel on Climate Change (IPCC) special report on Carbon Dioxide Capture and Storage*. Cambridge University Press, New York
Mishra M, Martin M, De Wit A. 2007. Miscible viscous fingering with linear adsorption on the porous matrix. *Phys. Fluids* 19:073101
Mishra M, Martin M, De Wit A. 2010a. Influence of miscible viscous fingering with negative log-mobility ratio on spreading of adsorbed analytes. *Chemical Engineering Science.* 65:2392–2398
Mishra M, Trevelyan P, Almarcha C, De Wit A. 2010b. Influence of double diffusive effects on

miscible viscous fingering. *Phys. Rev. Lett.* 105:204501
Mosheva E, Shmyrov A. 2017. Effect of the universal acid-base indicator on the formation of the concentration-dependent diffusion instability. *IOP Conf. Series: Materials Science and Engineering* 208:012029
Nagatsu Y. 2015. Viscous fingering phenomena with chemical reactions. *Current Phys. Chem.* 5:52–63
Nagatsu Y, Bae SK, Kato Y, Tada Y. 2008a. Miscible viscous fingering with a chemical reaction involving precipitation. *Phys. Rev. E* 77:067302
Nagatsu Y, De Wit A. 2011. Viscous fingering of a miscible reactive $A + B \rightarrow C$ interface for an infinitely fast chemical reaction: Nonlinear simulations. *Phys. Fluids* 23:043103
Nagatsu Y, Hosokawa Y, Ueda T, Kato Y, Tada Y. 2008b. Miscible displacements with a chemical reaction in a capillary tube. *AIChE J.* 54:601–613
Nagatsu Y, Iguchi C, Matsuda K, Kato Y, Tada Y. 2010. Miscible viscous fingering involving viscosity changes of the displacing fluid by chemical reactions. *Phys. Fluids* 22:024101
Nagatsu Y, Ishii Y, Tada Y, De Wit A. 2014. Hydrodynamic fingering instability induced by a precipitation reaction. *Phys. Rev. Lett.* 113:024502
Nagatsu Y, Kondo Y, Kato Y, Tada Y. 2009. Effects of moderate Damköhler number on miscible viscous fingering involving viscosity decrease due to a chemical reaction. *J. Fluid Mech* 625:97–124
Nagatsu Y, Kondo Y, Kato Y, Tada Y. 2011. Miscible viscous fingering involving viscosity increase by a chemical reaction with moderate Damköhler number. *Phys. Fluids* 23:014109
Nagatsu Y, Matsuda K, Kato Y, Tada Y. 2007. Experimental study on miscible viscous fingering involving viscosity changes induced by variations in chemical species concentrations due to chemical reactions. *J. Fluid Mech.* 571:475–493
Nagatsu Y, Ueda T. 2001. Effects of reactant concentrations on reactive miscible viscous fingering. *AIChE J.* 47:1711
Nagatsu Y, Ueda T. 2003. Effects of finger-growth velocity on reactive miscible viscous fingering. *AIChE J.* 49:789
Nagatsu Y, Ueda T. 2004. Analytical study on effects of finger-growth velocity on reaction characteristics of reactive miscible viscous fingering by using a convection-diffusion-reaction model. *Chem. Eng. Sci.* 59:3817
Nasr-El-Din H, Khulbe K, Hornof V, Neale G. 1990. Effects of interfacial reaction on the radial displacement of oil by alkaline solutions. *Rev. Inst. Fr. Pétr.* 45:231
Neufeld JA, Hesse M, Riaz A, Hallworth MA, Tchelepi HA, Huppert HE. 2010. Convective dissolution of carbon dioxide in saline aquifers. *Geophys. Res. Lett.* 37:L22404
Niroobakhsh Z, Litman M, Belmonte A. 2017. Flow instabilities due to the interfacial formation of surfactant-fatty acid material in a Hele-Shaw cell. *Phys. Rev. E* 96:053102
Outeda R, El Hasi C, D′Onofrio A, Zalts A. 2014. An experimental study of linear and nonlinear regimes of density-driven instabilities induced by CO_2 dissolution in water. *Chaos* 24:013135
Podgorski T, Sostarecz MC, Zorman S, Belmonte A. 2007. Fingering instabilities of a reactive micellar interface. *Phys. Rev. E* 79:016202
Radko T. 2013. Double diffusive convection. Cambridge University Press
Rana C, De Wit A. 2019. Oscillating viscous fingering. *Chaos*
Rana C, De Wit A, Martin M, Mishra M. 2014. Combined influences of viscous fingering and solvent effect on the distribution of adsorbed solutes in porous media. *RSC Advances* 4:34369
Rana C, Mishra M, De Wit A. 2018. Effect of anti-Langmuir adsorption on spreading in porous media. *Europhys. Lett.* 124:64003
Riaz A, Hesse M, Tchelepi HA, Orr Jr FM. 2006. Onset of convection in a gravitationally unstable diffusive boundary layer in porous media. *J. Fluid Mech.* 548:87–111
Riolfo LA, Nagatsu Y, Iwata S, Maes R, Trevelyan PMJ, De Wit A. 2012. Experimental evidence of reaction-driven miscible viscous fingering. *Phys. Rev. E* 85:015304(R)
Ritchie L, Pritchard D. 2011. Natural convection and the evolution of a reactive porous medium.

J. Fluid Mech. 673:286–317

Rongy L, Trevelyan P, De Wit A. 2008. Dynamics of A+B→C reaction fronts in the presence of buoyancy-driven convection. *Phys. Rev. Lett.* 101:084503

Rongy L, Trevelyan P, De Wit A. 2010. Influence of buoyancy-driven convection on the dynamics of A+B→C reaction fronts in horizontal solution layers. *Chem. Eng. Sci.* 65:2382–2391

Rose H, Britton M. 2013. Magnetic resonance imaging of reaction-driven viscous fingering in a packed bed. *Microporous and Mesoporous Materials* 178:64–68

Rousseaux G, De Wit A, Martin M. 2007. Viscous fingering in packed chromatographic columns: Linear stability analysis. *Journal of Chromatography A* 1149:254–273

Rousseaux G, Martin M, De Wit A. 2011. Viscous fingering in packed chromatographic columns: Non-linear dynamics. *Journal of Chromatography A* 1218:8353–8361

Sabet N, Hassanzadeh H, Abedi J. 2017. Control of viscous fingering by nanoparticles. *Phys. Rev. E* 96:063114

Sabet N, Raad S, Hassanzadeh H, Abedi J. 2018. Dynamics of miscible nanocatalytic reactive flows in porous media. *Phys. Rev. Applied* 10:054033

Saffman PG, Taylor GI. 1958. The penetration of a fluid into a porous medium or Hele-Shaw cell containing a more viscous liquid. *Proc. R. Soc. Lond. A* 245:312–329

Schuszter G, Brau F, De Wit A. 2014. Calcium carbonate mineralization in a confined geometry. *Environm. Sci. Techn. Lett.* 3:156–159

Schwarzenberger K, Eckert K, Odenbach S. 2012. Relaxation oscillations between Marangoni cells and double diffusive fingers in a reactive liquid-liquid system. *Chem. Eng. Sci.* 68:530–540

Sharma V, Pramanik S, Chen CY, Mishra M. 2019. A numerical study on reaction-induced radial fingering instability. *J. Fluid Mech.* 862:624–638

Slim AC. 2014. Solutal-convection regimes in a two-dimensional porous medium. *J. Fluid Mech.* 741:461–491

Slim AC, Bandi MM, Miller JC, Mahadevan L. 2013. Dissolution-driven convection in a Hele–Shaw cell. *Phys. Fluids* 25:024101

Stewart S, Marin D, Tullier M, Pojman J, Meiburg E, Bunton P. 2018. Stabilization of miscible viscous fingering by a step growth polymerization reaction. *Exp. in Fluids* 59:114

Swernath S, Pushpavanam S. 2007. Viscous fingering in a horizontal flow through a porous medium induced by chemical reactions under isothermal and adiabatic conditions. *J. Chem. Phys.* 127:204701

Swernath S, Pushpavanam S. 2008. Instability of a vertical chemical front: Effect of viscosity and density varying with concentration. *Phys. Fluids* 20:012101

Szymczak P, Ladd AJC. 2014. Reactive-infiltration instabilities in rocks. part 2. dissolution of a porous matrix. *J. Fluid Mech.* 738:591–630

Tanoue K, Ikemoto H, Yoshitomi M, Nishimura T. 2009a. Instabilized heat and mass transfer in exothermic chemically reacting flows. *Thermal Science and Engineering* 17:121–129

Tanoue K, Yoshitomi M, Nishimura T. 2009b. Heat transfer under buoyancy-induced flow at the chemical reaction front using thermochromic liquid crystal sheet. *J. Chem. Eng. Japan* 42:255–258

Thomas C, Dehaeck S, De Wit A. 2018. Convective dissolution of CO_2 in water and salt solutions. *Int. J. Greenhouse Gas Control* 72:105–116

Thomas C, Dehaeck S, De Wit A. 2019. Effect of precipitation mineralization reactions on convective dissolution of CO_2: an experimental study. *Phys. Rev. Fluids (submitted)*

Thomas C, Lemaigre L, Zalts A, D′Onofrio A, De Wit A. 2015. Experimental study of CO_2 convective dissolution: The effect of colour indicators. *Int. J. Greenhouse Gas Control* 42:525–533

Thomas C, Loodts V, Rongy L, De Wit A. 2016. Convective dissolution of CO_2 in reactive alkaline solutions: Active role of spectator ions. *Int. J. Greenhouse Gas Control* 53:230–242

Tiani R, De Wit A, Rongy L. 2018. Surface tension and buoyancy-driven flows across horizontally propagating chemical fronts. *Adv. Colloid Interface Sci.* 225:76

Trevelyan P, Walker A. 2018. Asymptotic properties of radial A+B→C reaction fronts. *Phys. Rev. E* 98:032118

Trevelyan PMJ, Almarcha C, De Wit A. 2011. Buoyancy-driven instabilities of miscible two-layer stratifications in porous media and Hele-Shaw cells. *J. Fluid Mech.* 670:38–65

Trevelyan PMJ, Almarcha C, De Wit A. 2015. Buoyancy-driven instabilities around miscible A+B→C reaction fronts: a general classification. *Phys. Rev. E* 91:023001

Tsuzuki R, Ban T, Fujimura M, Nagatsu Y. 2019. Dual role of surfactant-producing reaction in immiscible viscous fingering evolution. *Phys. Fluids* 31:022102

Turner J. 1979. Buoyancy effects in fluids. Cambridge University Press

Ward TJ, Cliffe KA, Jensen OE, Power H. 2014. Dissolution-driven porous-medium convection in the presence of chemical reaction. *J. Fluid Mech.* 747:316–349

White A, Ward T. 2012. Co_2 sequestration in a radial Hele-Shaw cell via an interfacial chemical reaction. *Chaos* 22:037114

Wooding RA. 1969. Growth of fingers at an unstable diffusing interface in a porous medium or Hele-Shaw cell. *J. Fluid Mech.* 39:477–495

Wylock C, Dehaeck S, Cartage T, Colinet P, Haut B. 2011. Experimental study of gas-liquid mass transfer coupled with chemical reactions by digital holographic interferometry. *Chem. Eng. Sc.* 66:3400–3412

Wylock C, Dehaeck S, Rednikov A, Colinet P. 2008. Chemo-hydrodynamical instability created by CO_2 absorption in an aqueous solution of $NaHCO_3$ and Na_2CO_3. *Microgravity Science and Technology* 20:171

Wylock C, Rednikov A, Haut B, Colinet P. 2014. Nonmonotonic Raleigh-Taylor instabilities driven by gas-liquid CO_2 chemisorption. *J. Phys. Chem. B* 118:11323–11329

Zalts A, El Hasi C, Rubio D, Urena A, D'Onofrio A. 2008. Pattern formation driven by an acid-base neutralization reaction in aqueous media in a gravitational field. *Phys. Rev. E* 77:015304(R)